ASC Report No. 24/2012

Numerical Solution of a Second-Order Initial Value Problem Describing Flow in Concrete

P. Amodio, Ch. Budd, O. Koch, G. Settanni, and E.B. Weinmüller

Institute for Analysis and Scientific Computing
Vienna University of Technology — TU Wien
www.asc.tuwien.ac.at ISBN 978-3-902627-05-6

Most recent ASC Reports

23/2012 *D. Stürzer, A. Arnold*
Spectral analysis and long-time behaviour of a Fokker-Planck equation with a non-local perturbation

22/2012 *M. Bessemoulin-Chatard and A. Jüngel*
A finite volume scheme for a Keller-Segel model with additional cross-diffusion

21/2012 *M. Bulatov, P. Lima, E. Weinmüller*
Existence and Uniqueness of Solutions to Weakly Singular Integral-Algebraic and Integro-Differential Equations

20/2012 *M. Karkulik, G. Of, and D. Praetorius*
Convergence of adaptive 3D BEM for weakly singular integral equations based on isotropic mesh-refinement

19/2012 *A. Jüngel, René Pinnau, and E. Röhrig*
Existence analysis for a simplified transient energy-transport model for semiconductors

18/2012 *I. Rachunková, A. Spielauer, S. Staněk and E.B. Weinmüller*
The structure of a set of positive solutions to Dirichlet BVPs with time and space singularities

17/2012 *J.-F. Mennemann, A. Jüngel, and H. Kosina*
Transient Schrödinger-Poisson simulations of a high-frequency resonant tunneling diode oscillator

16/2012 *N. Zamponi and A. Jüngel*
Two spinorial drift-diffusion models for quantum electron transport in graphene

15/2012 *M. Aurada, M. Feischl, T. Führer, M. Karkulik, D. Praetorius*
Efficiency and optimality of some weighted-residual error estimator for adaptive 2D boundary element methods

14/2012 *I. Higueras, N. Happenhofer, O. Koch, and F. Kupka*
Optimized Imex Runge-Kutta methods for simulations in astrophysics: A detailed study

Institute for Analysis and Scientific Computing
Vienna University of Technology
Wiedner Hauptstraße 8–10
1040 Wien, Austria

E-Mail: admin@asc.tuwien.ac.at
WWW: http://www.asc.tuwien.ac.at
FAX: +43-1-58801-10196

ISBN 978-3-902627-05-6

© Alle Rechte vorbehalten. Nachdruck nur mit Genehmigung des Autors.

ASC TU WIEN

Numerical Solution of a Second-Order Initial Value Problem Describing Flow in Concrete

P. Amodio, Ch. Budd, O. Koch, G. Settanni, and E.B. Weinmüller

July 22, 2012

1 Introduction

A model for the time dependent flow of water through a variably saturated porous medium with exponential diffusivity, such as soil, rock or concrete is given by

$$\frac{\partial u}{\partial t} = \frac{\partial}{\partial x}\left(D(u)\frac{\partial u}{\partial x}\right), \tag{1}$$

where $u(x,t)$ is the *saturation* and is the fraction by volume of the pore space occupied by the liquid a distance x into the porous medium, and

$$D(u) = D_0 e^{\beta u}.$$

In this problem the bulk of the liquid resides in the interval $x \in [0, x^*(t)]$ where the moving interface $x^*(t)$ is called the *wetting front*, and $u \ll 1$ if $x > x^*$. The physical derivation of this equation is given in [6], [9], [10]. The numerical treatment of this problem was first discussed in [12]. A comprehensive overview of numerical methods for flow in porous media is given for instance in [8]. In the present paper we do not focus on a simulation of the full model, but adopt a numerical approach to investigate the asymptotical behavior of *self-similar solutions* of the equation (1), which are stable attractors and take the form

$$u(x,t) = \psi(y), \quad y = x/t^{1/2}, \quad 0 < y < \infty.$$

If we set

$$\theta(y) = e^{\beta\psi(y)}$$

and make a trivial rescaling, it then follows that $\theta(y)$ satisfies the ordinary differential equation problem

$$\theta(y)\theta_{yy}(y) = -y\theta_y(y), \quad \theta_y(0) = -\gamma = -\gamma(\beta) < 0, \quad \theta(0) = 1, \quad y > 0. \tag{2}$$

The purpose of this paper is to make a numerical study of the solutions of (2) in the limit of large γ which corresponds to a problem with $\beta \gg 1$ with large diffusion when u is not small.

The resulting problem is a scalar second order initial value problem describing the flow of the wetting front. The difficulty lies in the fact that at the beginning of the integration interval the values of the first and second derivative of the solution become extremely large forcing immense step size reduction of any numerical method applied to solve the problem. The idea of discretizing each derivative of the solution by means of finite difference schemes has been extensively used in the past. In [3] and later in [1, 2, 4], the authors proposed to apply high order finite difference schemes for the solution of BVPs in ODEs, following the idea inherited by the BVMs, see [5]. Especially, different formulae with the same order have been proposed for the points at the beginning and at the end of the grid.

The main advantages of this approach derive from the fact that the vector of unknowns contains only the solution values. This choice, on one hand, reduces the computational cost of the algorithm when compared with the approach in which the transformation of the second order formulation to the first order one is carried out. In this case, the solution vector of the first order system contains both, the solution and its first derivative. On the other hand, our approach simplifies the step size adaptation procedure and allows the final discrete system to become fully implicit. Moreover, there is complete freedom in the choice of the schemes approximating each derivative which could not only depend on the problem, but also on the discretization points.

In [2] the same idea is applied to IVPs for ODEs. Two approaches are proposed to discretize the first derivative in the initial point: we can choose to approximate the ODE using a formula including only the solution values, or to define difference schemes which also use the values of the first derivative in the first point. As a general belief, the second approach seems to be preferable. However, for the *flow in concrete* problem, since the values of the first derivative are very strongly influencing the solution behavior, and therefore immensely affect the step size variation, the first type of schemes is used.

2 Asymptotical properties: Part 1

The aim of the following sections is to verify by numerical computations asymptotical results for the problem (3) which have been derived for $\gamma \to \infty$ in [7]. The computational results given below have been carried out on the basis of the preprint [7]. Using finite difference schemes (see Section 6 for details), we have first solved the initial value problem,

$$\theta\theta_{yy} = -y\theta_y, \quad \theta_y(0) = -\gamma, \quad \theta(0) = 1, \tag{3}$$

for $\gamma = 2, 3, \ldots, 15$ and for $\gamma = 18$ (for $\gamma > 18$ the solution in the last points is too small to be computed accurately and for $\gamma > 26$ it is smaller than the smallest positive double precision machine number). We have considered methods

of orders equal to $4, 6, 8$, and 10 to understand how the order of the numerical method influences the accuracy of the approximate solutions. As a general remark, we observe that the discretization errors are larger than the round-off errors of the floating point operations. Moreover, we step forward using variable stepsizes, and for a fixed tolerance, methods of higher order require smaller mesh size but they do not necessarily achieve better precision. This is most probably due to the fact that higher derivatives are extremely unsmooth.

The purpose of the following investigations is to numerically verify asymptotic results derived in [7]. For all theoretical claims stated below we refer the reader to this reference.
The solution has been calculated on finite intervals $[0, y_\infty]$, with the interval endpoint $y_\infty = 10, 20, 30, 40, 50$, to see how strongly the value of $\theta(y_\infty)$ depends on the length of the interval of integration. It turns out that, especially for large values of γ, the influence of the interval length is not very strong, see Table 1. Therefore, from now on, we use the interval $[0, 10]$ and $\theta(\infty) = \theta_\infty := \theta(10)$ for all calculations.

The following description refers to the data in Tables 2 and 3. All data are given for $\gamma = 2, 6, 10, 18$. Since the reference values are given by the asymptotics for large values of γ, we expect to see their accuracy improving for growing γ.

In rows 1 and 2, we specify the values of θ_∞ and y^*. Note that y^* is the point where θ_{yy} takes its maximal value in the interval $[0, y_\infty] = [0, 10]$.

Since θ_∞ satisfies the relation [7],

$$\log(\theta_\infty) = -\gamma^2 - \frac{1}{2} + \frac{\alpha}{\gamma^2}, \tag{4}$$

we first report the relative error in approximating $-\log(\theta_\infty)$ by $\gamma^2 + \frac{1}{2}$ (row 3) and then compute an approximation for α (row 4). Row 3 confirms that the value of θ_∞ has been computed accurately (the relative error is always smaller than γ^{-4}) and $\alpha \approx -0.08$.

Also y^* needs to satisfy [7],

$$y^* = \frac{1}{\gamma} + \frac{1}{2\gamma^3} + \frac{\beta}{\gamma^5}, \tag{5}$$

which we compare with the numerical value. We first use

$$y^* = \frac{1}{\gamma} + \frac{s^*}{\gamma^3} \tag{6}$$

in order to obtain

$$s^* = \gamma^3 y^* - \gamma^2 = \frac{1}{2} + O\left(\frac{1}{\gamma^2}\right). \tag{7}$$

In row 5, we specify the relative error $|s^* - 0.5|/0.5$ and then use (5) to approximate β (row 6). Again the relative error is smaller than γ^{-2} while the value of β seems to oscillate around 0.95.

We now try to verify results describing the values of $\theta(y^*)$ and $\theta_{yy}(y^*)$ [7],

$$\theta(y^*) = e\theta_\infty, \tag{8a}$$

$$\theta_{yy}(y^*) = \hat{\theta}_{yy} \equiv \frac{e^{\gamma^2 - 1/2}}{\gamma^2}. \tag{8b}$$

Rows 7 and 8 contain the values of $\theta(y^*)$ and $\theta_{yy}(y^*)$. In rows 9 and 10 we specify the relative errors,

$$\frac{|\theta(y^*) - e\theta_\infty|}{e\theta_\infty}, \quad \frac{\left|\theta_{yy}(y^*) - \hat{\theta}_{yy}\right|}{\hat{\theta}_{yy}}, \tag{9}$$

respectively. While for (8b) row 10 suggests that $\theta_{yy}(y^*) = \hat{\theta}_{yy} + O(\gamma^{-2})$, for (8a) row 9 only shows a good approximation whose quality increases with larger γ.

Finally we use the relation [7],

$$\theta\left(\frac{1}{\gamma}\right) = \frac{1}{2\gamma^2} - \frac{\log(\gamma)}{\gamma^4} + \frac{b}{\gamma^4}, \tag{10}$$

to estimate the value of b given by the known approximation

$$\hat{b} = \frac{11}{12} - \frac{1}{2}\log(2) = 0.5700930763866940.$$

Rows 11 and 12 contain the numerical value of b and the relative error, respectively.

$\gamma = 6$					
order	$\theta(10)$	$\theta(20)$	$\theta(30)$	$\theta(40)$	$\theta(50)$
4	1.403505547530107e−016	1.403505547530106e−016	1.403505547530108e−016	1.403505547530108e−016	1.403505547530107e−016
6	1.403505498068323e−016	1.403505498068323e−016	1.403505498068321e−016	1.403505498068323e−016	1.403505498068324e−016
8	1.403505497221929e−016	1.403505497221926e−016	1.403505497221936e−016	1.403505497221929e−016	1.403505497221933e−016
10	1.403505492946673e−016	1.403505492946662e−016	1.403505492946644e−016	1.403505492946654e−016	1.403505492946670e−016

$\gamma = 10$					
order	$\theta(10)$	$\theta(20)$	$\theta(30)$	$\theta(40)$	$\theta(50)$
4	2.254440321030590e−044	2.254440321030590e−044	2.254440321030590e−044	2.254440321030590e−044	2.254440321030590e−044
6	2.254439910312038e−044	2.254439910312031e−044	2.254439910312040e−044	2.254439910312037e−044	2.254439910312035e−044
8	2.254439903035485e−044	2.254439903035499e−044	2.254439903035495e−044	2.254439903035496e−044	2.254439903035494e−044
10	2.254439870668035e−044	2.254439870667992e−044	2.254439870668041e−044	2.254439870667989e−044	2.254439870668002e−044

$\gamma = 14$					
order	$\theta(10)$	$\theta(20)$	$\theta(30)$	$\theta(40)$	$\theta(50)$
4	4.580879628543622e−086	4.580879628543621e−086	4.580879628543624e−086	4.580879628543621e−086	4.580879628543622e−086
6	4.580877107376558e−086	4.580877107376563e−086	4.580877107376567e−086	4.580877107376562e−086	4.580877107376554e−086
8	4.580877068174931e−086	4.580877068174953e−086	4.580877068174950e−086	4.580877068174946e−086	4.580877068174930e−086
10	4.580876883300804e−086	4.580876883300798e−086	4.580876883300863e−086	4.580876883300838e−086	4.580876883300735e−086

$\gamma = 18$					
order	$\theta(10)$	$\theta(20)$	$\theta(30)$	$\theta(40)$	$\theta(50)$
4	1.178498689884995e−141	1.178498689884996e−141	1.178498689884996e−141	1.178498689884995e−141	1.178498689884996e−141
6	1.178497263659187e−141	1.178497263659187e−141	1.178497263659186e−141	1.178497263659188e−141	1.178497263659188e−141
8	1.178497239286140e−141	1.178497239286134e−141	1.178497239286134e−141	1.178497239286137e−141	1.178497239286139e−141
10	1.178497080238536e−141	1.178497080238508e−141	1.178497080238496e−141	1.178497080238508e−141	1.178497080238530e−141

Table 1: Dependence of the terminal solution value θ_∞ on the interval length y_∞.

$\gamma = 2$				
Order	4	6	8	10
θ_∞	1.046797385732013e−002	1.046797384878747e−002	1.046797384984442e−002	1.046797384405275e−002
y^*	5.717469856837706e−001	5.717972928062153e−001	5.722758632712603e−001	5.722109401170057e−001
$\frac{\lvert\log(\theta_\infty)+\gamma^2+0.5\rvert}{\gamma^2+0.5}$	1.320773149055220e−002	1.320773167169027e−002	1.320773164925231e−002	1.320773177220246e−002
α	−2.377391668299396e−001	−2.377391700904248e−001	−2.377391696865416e−001	−2.377391718996442e−001
$\lvert s^*-0.5\rvert/0.5$	1.479517709403293e−001	1.487566848994444e−001	1.564138123401655e−001	1.553750418720910e−001
β	2.959035418806586e−001	2.975133697988888e−001	3.128276246803310e−001	3.107500837441819e−001
$\theta(y^*)$	2.526885480647071e−002	2.524231301750860e−002	2.499133353627827e−002	2.502522115040241e−002
$\theta_{yy}(y^*)$	1.194443737925854e+001	1.194443721622962e+001	1.194359539439109e+001	1.194379929416069e+001
$\frac{\lvert\theta(y^*)-e\theta_\infty\rvert}{e\theta_\infty}$	1.119683415385825e−001	1.129011076167978e−001	1.217213620005543e−001	1.205304379670169e−001
$\lvert\theta_{yy}(y^*)-\hat{\theta}_{yy}\rvert/\hat{\theta}_{yy}$	4.427630212213725e−001	4.427630015291861e−001	4.426613182618603e−001	4.426859472199501e−001
b	1.363248895993793e−001	1.363248888390932e−001	1.363248890283607e−001	1.363248870792130e−001
$\lvert b-\hat{b}\rvert/\hat{b}$	7.608725745918196e−001	7.608725759254370e−001	7.608725755934430e−001	7.608725790124421e−001

$\gamma = 6$				
Order	4	6	8	10
θ_∞	1.403505547530107e−016	1.403505498068323e−016	1.403505497221929e−016	1.403505492946673e−016
y^*	1.691107214202116e−001	1.691107214133044e−001	1.691107214134170e−001	1.691107214107735e−001
$\frac{\lvert\log(\theta_\infty)+\gamma^2+0.5\rvert}{\gamma^2+0.5}$	6.543612199557361e−005	6.543708751880879e−005	6.543710404097143e−005	6.543718749664911e−005
α	−8.598306430218372e−002	−8.598433299971475e−002	−8.598435470983645e−002	−8.598446437059693e−002
$\lvert s^*-0.5\rvert/0.5$	5.583165353139918e−002	5.583165054747497e−002	5.583165059613293e−002	5.583164945413444e−002
β	1.004969763565314e+000	1.004969709854734e+000	1.004969710730562e+000	1.004969690174517e+000
$\theta(y^*)$	3.818192860115130e−016	3.812030422586454e−016	3.795150040198615e−016	3.859609149820460e−016
$\theta_{yy}(y^*)$	7.496068191579922e+013	7.496068410014986e+013	7.495967250081973e+013	7.495571062508375e+013
$\frac{\lvert\theta(y^*)-e\theta_\infty\rvert}{e\theta_\infty}$	8.044913935855633e−004	8.107388822116135e−004	5.235334871455419e−003	1.166034925528076e−002
$\lvert\theta_{yy}(y^*)-\hat{\theta}_{yy}\rvert/\hat{\theta}_{yy}$	3.200528620288561e−002	3.200531627546967e−002	3.199138929629170e−002	3.193684501256429e−002
b	4.542757606068255e−001	4.542757162962778e−001	4.542757172349243e−001	4.542756983567393e−001
$\lvert b-\hat{b}\rvert/\hat{b}$	2.031550997144713e−001	2.031551774395824e−001	2.031551757931030e−001	2.031552089073185e−001

Table 2: Asymptotical results: Part 1.

$\gamma = 10$				
Order	4	6	8	10
θ_∞	2.254440321030590e−044	2.254439910312038e−044	2.254439903035485e−044	2.254439870668035e−044
y^*	1.005094588206025e−001	1.005094588173915e−001	1.005094588173695e−001	1.005094588166961e−001
$\frac{\lvert\log(\theta_\infty)+\gamma^2+0.5\rvert}{\gamma^2+0.5}$	8.381534862525284e−006	8.383347619373176e−006	8.383379735339227e−006	8.383522593173135e−006
α	−8.423442536837911e−002	−8.425264357470041e−002	−8.425296634015922e−002	−8.425440206139001e−002
$\lvert s^*-0.5\rvert/0.5$	1.891764120503581e−002	1.891763478295161e−002	1.891763473901165e−002	1.891763339222052e−002
β	9.458820602506902e−001	9.458817391464359e−001	9.458817369495821e−001	9.458816696103923e−001
$\theta(y^*)$	6.126853837541197e−044	6.112941093579158e−044	6.179228381160976e−044	6.241068630247245e−044
$\theta_{yy}(y^*)$	1.648468426869335e+041	1.648463633543453e+041	1.648412414631253e+041	1.648197595344220e+041
$\frac{\lvert\theta(y^*)-e\theta_\infty\rvert}{e\theta_\infty}$	2.203452148159067e−004	2.490444241387861e−003	8.326316736789704e−003	1.841742149797827e−002
$\lvert\theta_{yy}(y^*)-\hat{\theta}_{yy}\rvert/\hat{\theta}_{yy}$	1.106641417450169e−002	1.106347425115717e−002	1.103205980544998e−002	1.090030322297867e−002
b	5.138760976981811e−001	5.138757996757584e−001	5.138757975462900e−001	5.138757344251843e−001
$\lvert b-\hat{b}\rvert/\hat{b}$	9.861017615723677e−002	9.861069891822982e−002	9.861070265352932e−002	9.861081337423142e−002

$\gamma = 18$				
Order	4	6	8	10
θ_∞	1.178498689884995e−141	1.178497263659187e−141	1.178497239286140e−141	1.178497080238536e−141
y^*	5.564177918914028e−002	5.564177918825954e−002	5.564177918834908e−002	5.564177918801359e−002
$\frac{\lvert\log(\theta_\infty)+\gamma^2+0.5\rvert}{\gamma^2+0.5}$	7.913110850624213e−007	7.950405348276963e−007	7.951042681243711e−007	7.955201633050178e−007
α	−8.319686486129285e−002	−8.358897175071434e−002	−8.359567254206013e−002	−8.363939892956296e−002
$\lvert s^*-0.5\rvert/0.5$	5.712462132123619e−003	5.712451859267276e−003	5.712452903708254e−003	5.712448990493613e−003
β	9.254188654173835e−001	9.254172011994041e−001	9.254173704034648e−001	9.254167364749771e−001
$\theta(y^*)$	3.198906899145607e−141	3.209398993229446e−141	3.211721064871286e−141	3.220612538966346e−141
$\theta_{yy}(y^*)$	9.664468728333972e+137	9.664473940754825e+137	9.664458760222388e+137	9.664354974061130e+137
$\frac{\lvert\theta(y^*)-e\theta_\infty\rvert}{e\theta_\infty}$	1.431149209001307e−003	1.845268999181951e−003	2.570147096053791e−003	5.345843389674220e−003
$\lvert\theta_{yy}(y^*)-\hat{\theta}_{yy}\rvert/\hat{\theta}_{yy}$	3.363040886020695e−003	3.363582038419761e−003	3.362005998844594e−003	3.351230942161327e−003
b	5.471501619326116e−001	5.471485474696558e−001	5.471487116780027e−001	5.471480869323990e−001
$\lvert b-\hat{b}\rvert/\hat{b}$	4.024415556753806e−002	4.024698749625749e−002	4.024669945847258e−002	4.024779532444529e−002

Table 3: Asymptotical results: Part 1 continued.

3 Solution graphs

In Figures 1, 3, and 5, we show the graphs (logarithmic scale) of the numerical solution and its first and second derivative for the values $\gamma = 4, 10$ and 18. Moreover, in Figures 2, 4, and 6 we plot the variation of the step sizes for the methods of orders 4, 6, 8, and 10. The tolerance used is 1e−12 and the initial step size is 1e−3.
The approximation of the first and the second derivative becomes unreliable in the area where the solution is close to the asymptotic value zero.

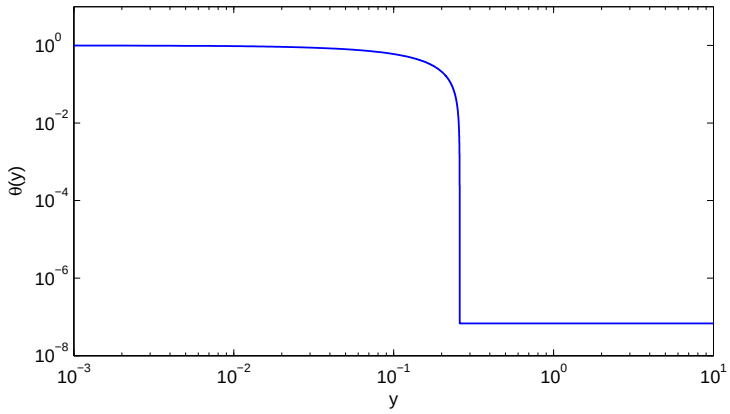

(a) *Numerical solution.*

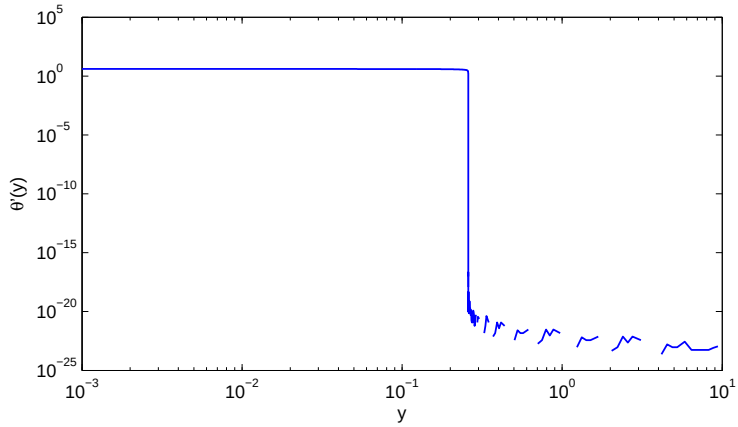

(b) *Numerical approximation of the absolute value of the first derivative.*

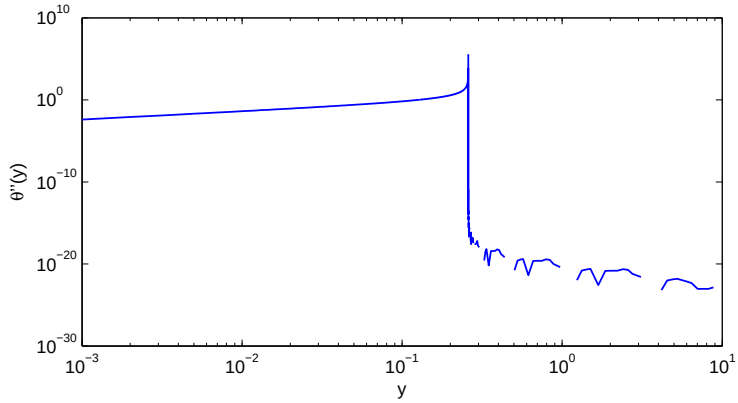

(c) *Numerical approximation of the absolute value of the second derivative.*

Figure 1: $\gamma = 4$.

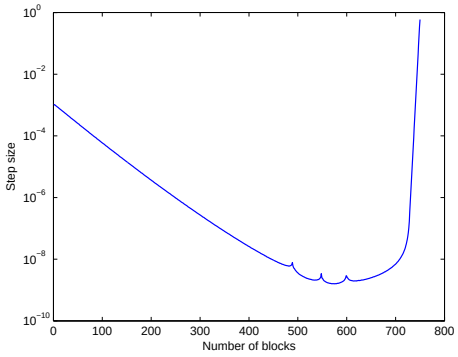

(a) order = 4.

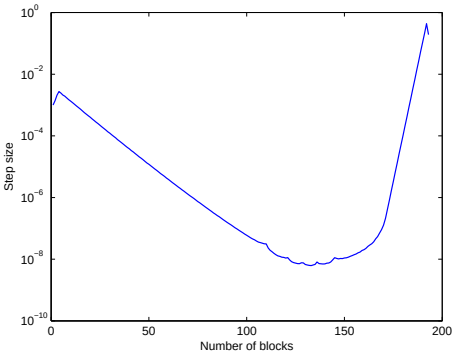

(b) order = 6.

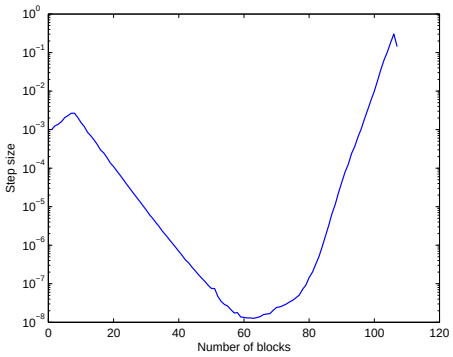

(c) order = 8.

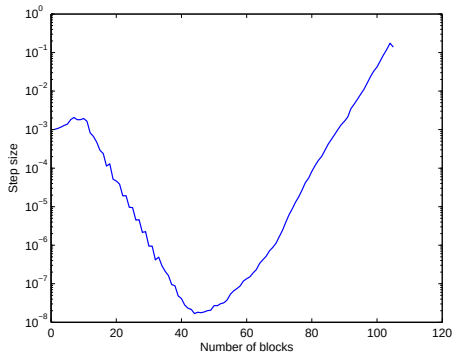

(d) order = 10.

Figure 2: Step size variation for each block, $\gamma = 4$.

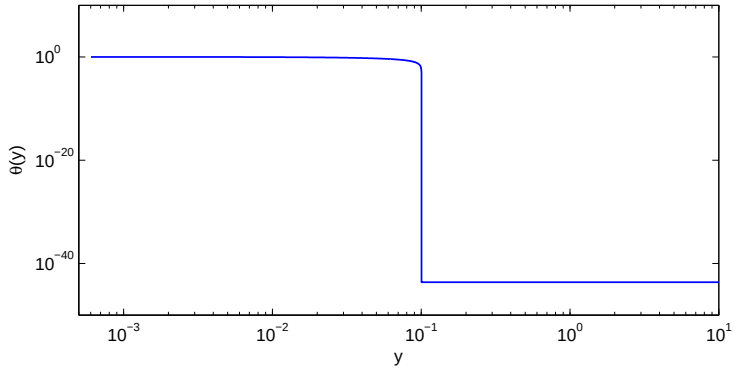

(a) *Numerical solution.*

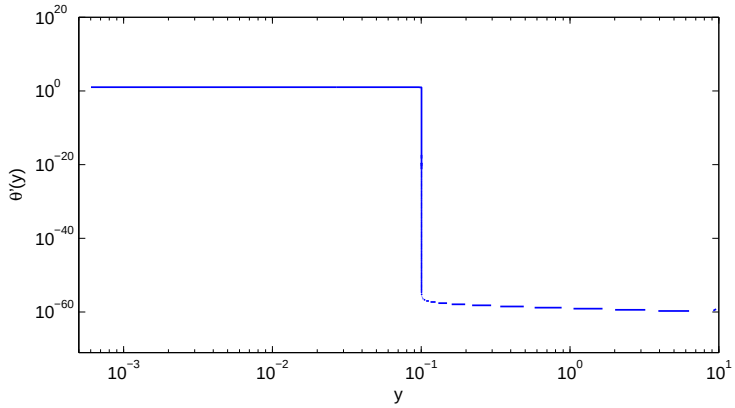

(b) *Numerical approximation of the absolute value of the first derivative.*

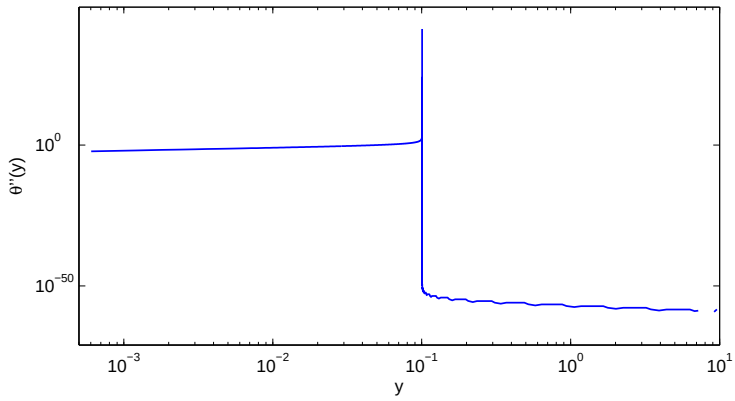

(c) *Numerical approximation of the absolute value of the second derivative.*

Figure 3: $\gamma = 10$.

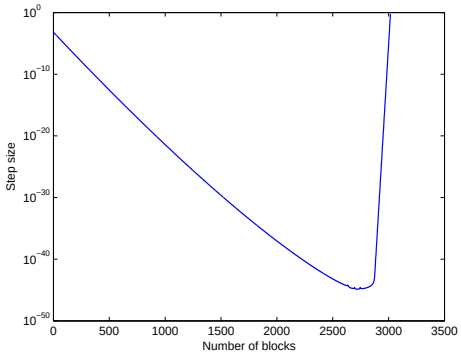

(a) order = 4.

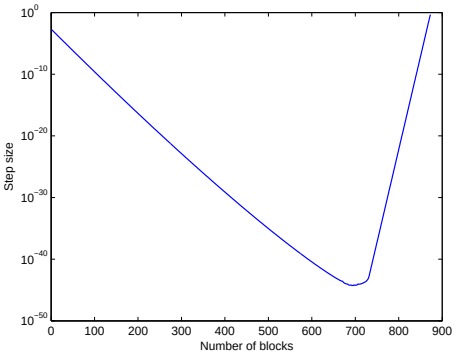

(b) order = 6.

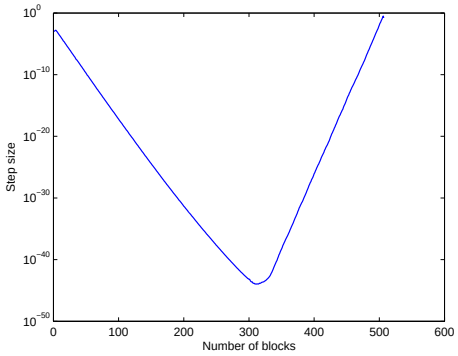

(c) order = 8.

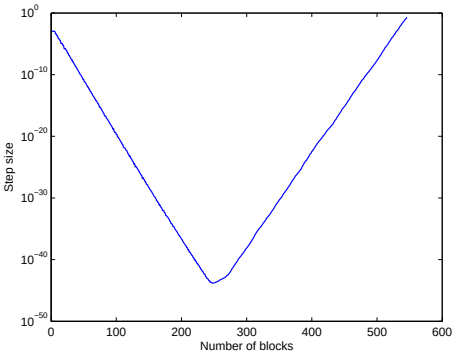

(d) order = 10.

Figure 4: Step size variation for each block, $\gamma = 10$.

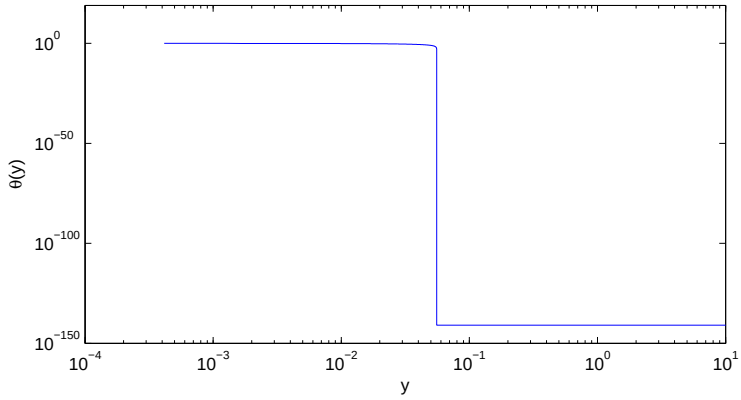

(a) *Numerical solution.*

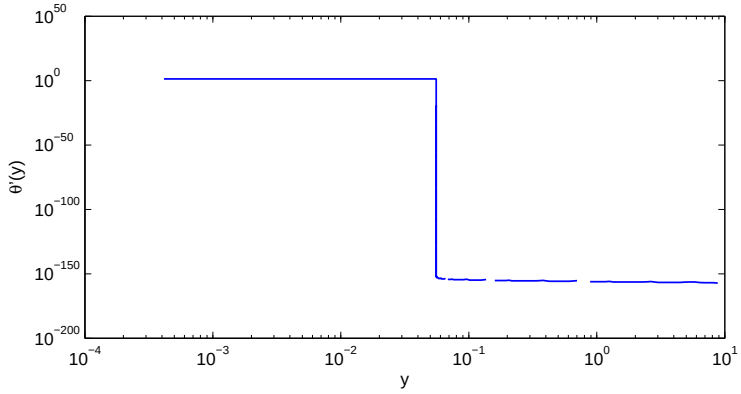

(b) *Numerical approximation of the absolute value of the first derivative.*

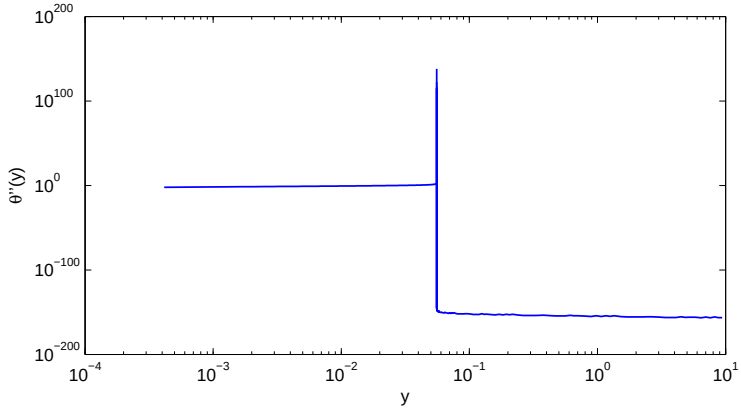

(c) *Numerical approximation of the absolute value of the second derivative.*

Figure 5: $\gamma = 18$.

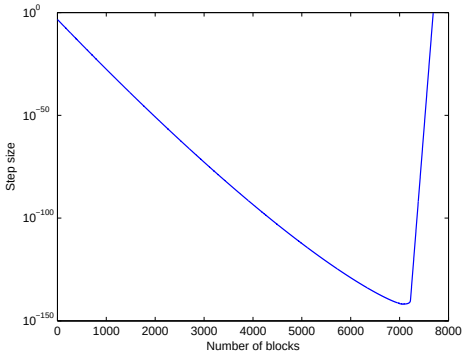

(a) order = 4.

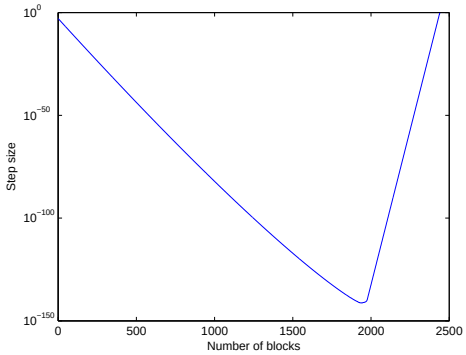

(b) order = 6.

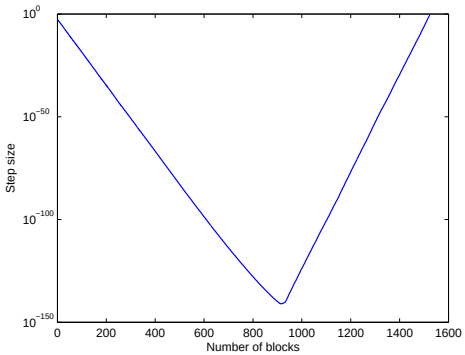

(c) order = 8.

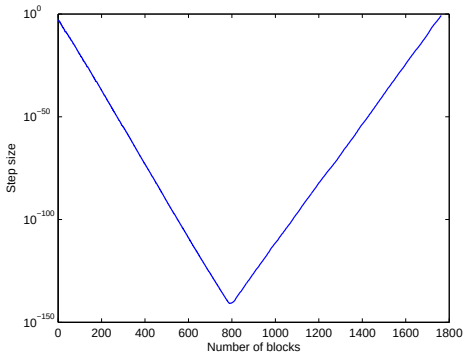

(d) order = 10.

Figure 6: Step size variation for each block, $\gamma = 18$.

4 Asymptotical properties: Part 2 – Mid-range calculation, $s < 0$

As the first part of our discussion of the case where $|s|$ is in the mid-range between 1 and γ^2, we consider negative s.
Case 1: $1 \ll |s| \ll \gamma^2, \;\; s < 0$

Let $-\gamma^2 \ll s \ll -1$. From [7],

$$y(s) = \frac{1}{\gamma} + \frac{s}{\gamma^3}, \tag{11}$$

so we obtain s as

$$s = \gamma^3 y - \gamma^2, \tag{12}$$

and consequently, we can approximate the values of $v(s)$ by

$$v(s) = \gamma^4 \theta(y). \tag{13}$$

For the calculations, we choose the points y such that s are in the interval $[-\gamma^2, -1]$, i.e., $0 \ll y \ll \frac{1}{\gamma} - \frac{1}{\gamma^3}$, and compute $\theta(y)$.

From [7],

$$v(s) = \gamma^2 v_0(s) + v_1(s) + O\left(\frac{1}{\gamma^2}\right), \tag{14}$$

holds, where

$$v_0(s) = \frac{1}{2} - s. \tag{15}$$

From (14) and (15), we obtain the numerical approximation for the values of $v_1(s)$,

$$v_1(s) = v(s) - \gamma^2 v_0(s) + O\left(\frac{1}{\gamma^2}\right) = v(s) - \gamma^2\left(\frac{1}{2} - s\right) + O\left(\frac{1}{\gamma^2}\right). \tag{16}$$

Furthermore, the asymptotical values of $v_1(s)$ are available [7],

$$\begin{aligned} v_1(s) \quad &= (c-2)\log(\gamma)s + \left(d - \frac{1}{2}\right)s + a\log(\gamma) + b - \\ &\quad - \left(s - \frac{1}{2}\right)\log\left(\frac{1}{2} - s\right) + s - \frac{\log(1/2)}{2}, \end{aligned} \tag{17}$$

where $a = -1$, $b = \dfrac{11}{12} - \dfrac{1}{2}\log(2)$, $c = 4$, $d = -\dfrac{1}{2}$.

In Figures 7 to 12, we plot the values of $v_1(s)$ and their numerical approximations together with the relative errors (logarithmic scale).

One observes the desired asymptotical behaviour for points s such that $-\gamma^2 \ll s$ and large values of γ.

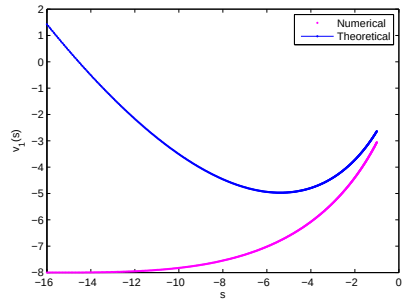

(a) $\gamma = 4$.

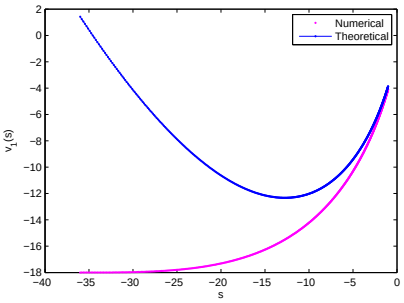

(b) $\gamma = 6$.

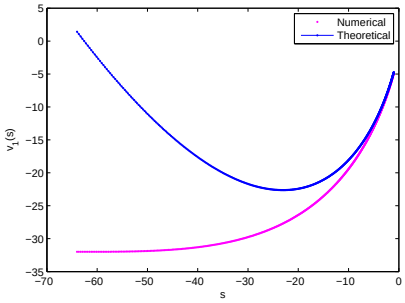

(c) $\gamma = 8$.

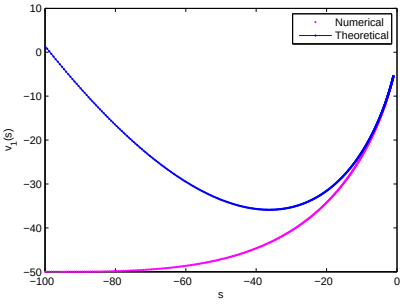

(d) $\gamma = 10$.

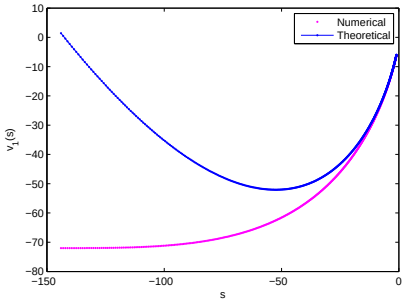

(e) $\gamma = 12$.

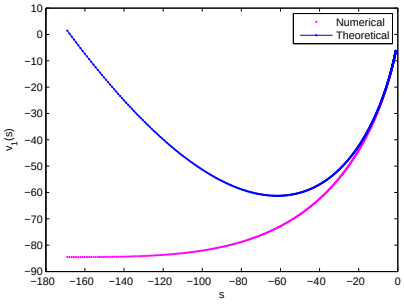

(f) $\gamma = 13$.

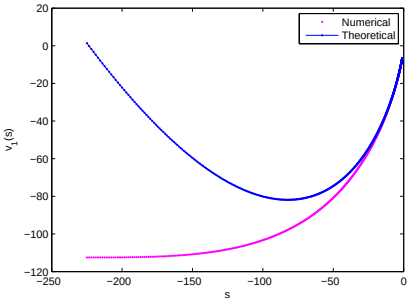

(g) $\gamma = 15$.

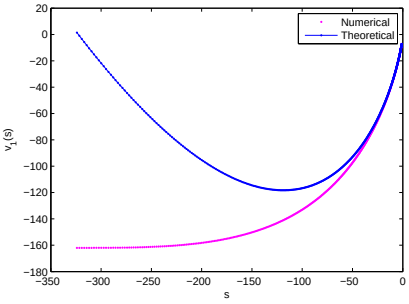

(h) $\gamma = 18$.

Figure 7: Analytical values and numerical approximation for v_1, order 4.

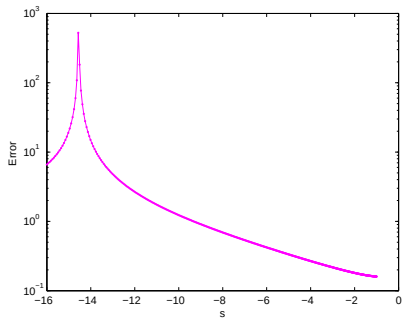

(a) $\gamma = 4$.

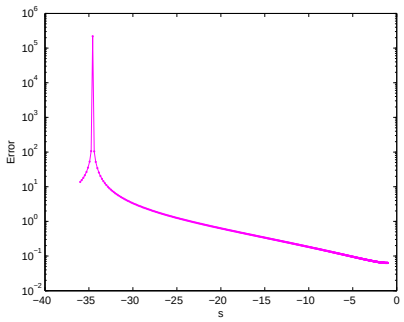

(b) $\gamma = 6$.

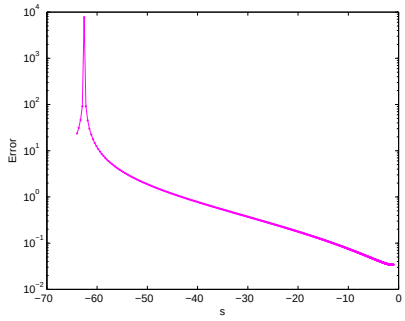

(c) $\gamma = 8$.

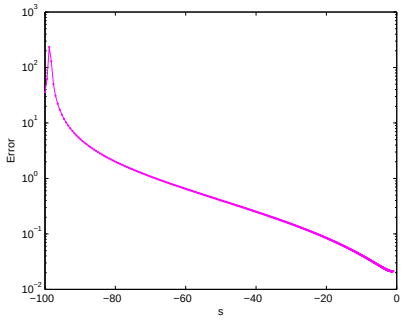

(d) $\gamma = 10$.

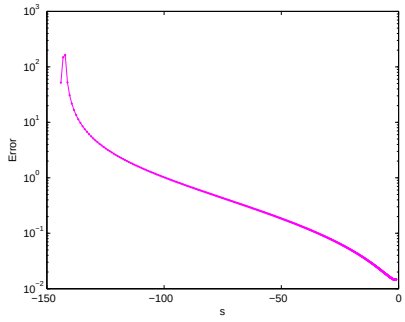

(e) $\gamma = 12$.

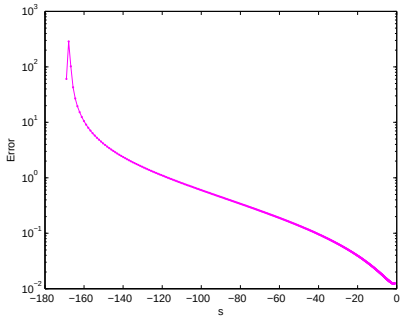

(f) $\gamma = 13$.

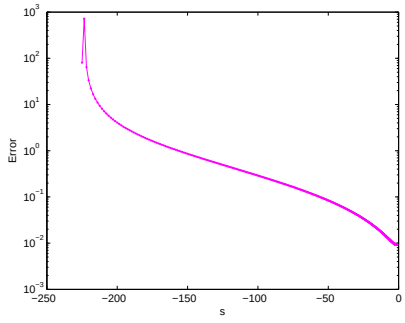

(g) $\gamma = 15$.

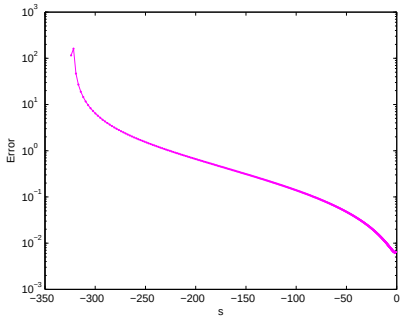

(h) $\gamma = 18$.

Figure 8: Relative error of v_1, order 4.

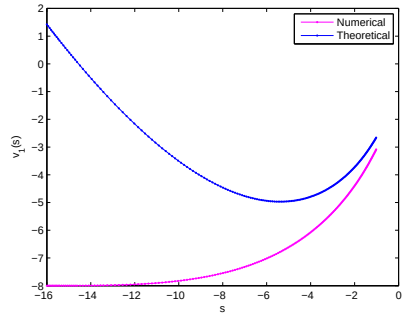

(a) $\gamma = 4$.

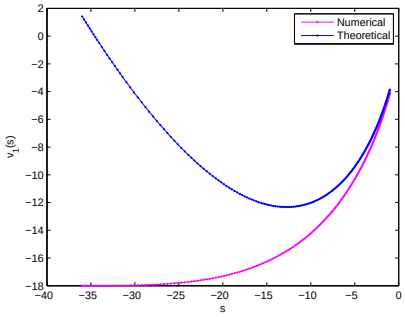

(b) $\gamma = 6$.

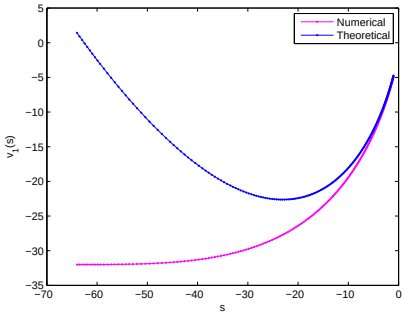

(c) $\gamma = 8$.

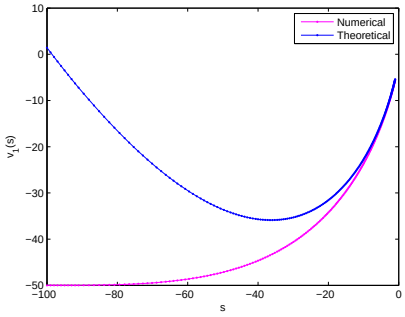

(d) $\gamma = 10$.

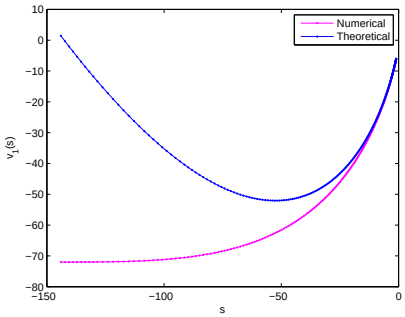

(e) $\gamma = 12$.

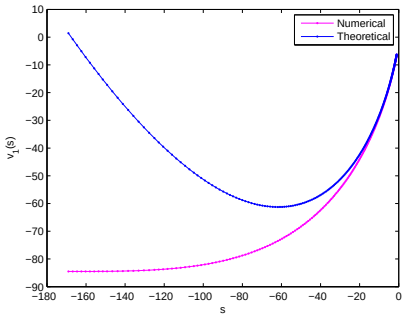

(f) $\gamma = 13$.

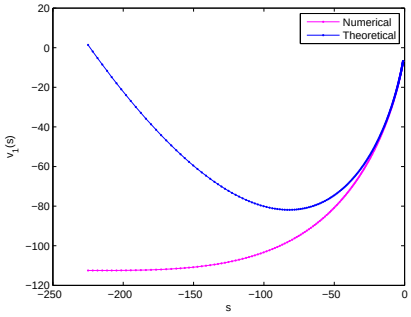

(g) $\gamma = 15$.

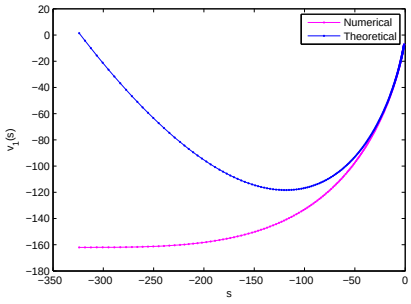

(h) $\gamma = 18$.

Figure 9: Analytical values and numerical approximation for v_1, order 6.

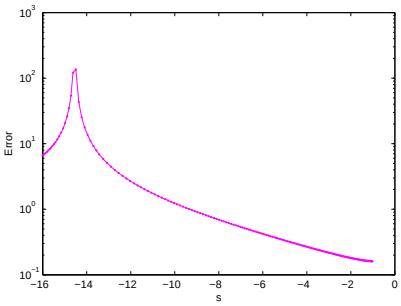

(a) $\gamma = 4$.

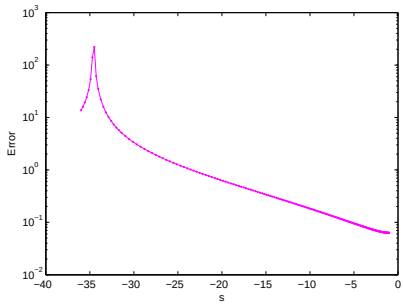

(b) $\gamma = 6$.

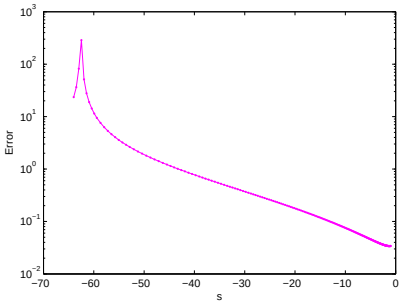

(c) $\gamma = 8$.

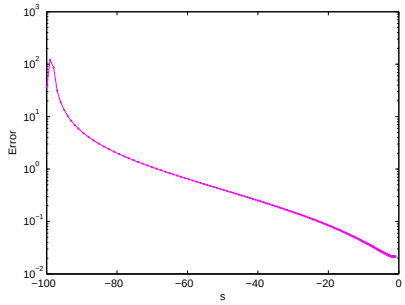

(d) $\gamma = 10$.

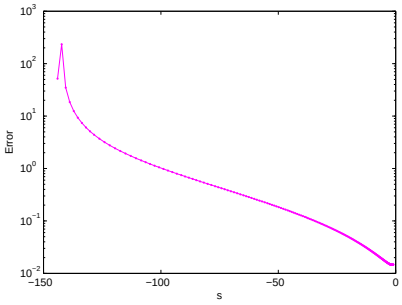

(e) $\gamma = 12$.

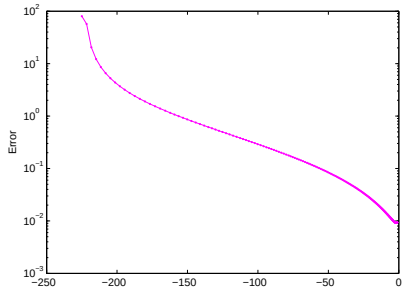

(f) $\gamma = 13$.

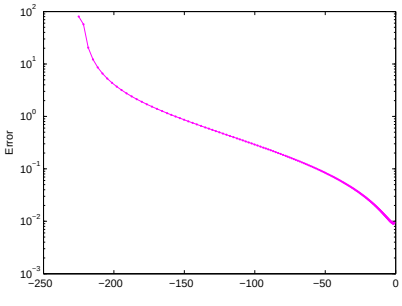

(g) $\gamma = 15$.

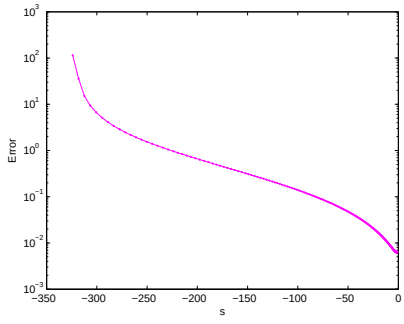

(h) $\gamma = 18$.

Figure 10: Relative error of v_1, order 6.

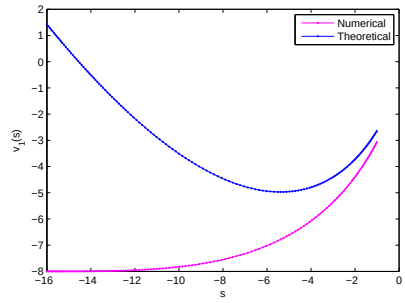

(a) $\gamma = 4$.

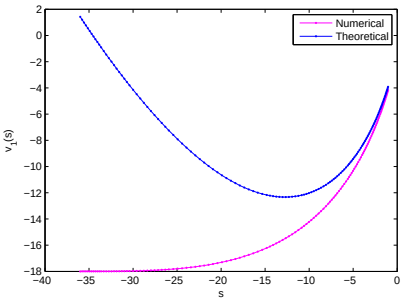

(b) $\gamma = 6$.

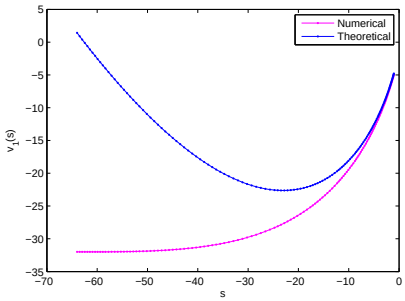

(c) $\gamma = 8$.

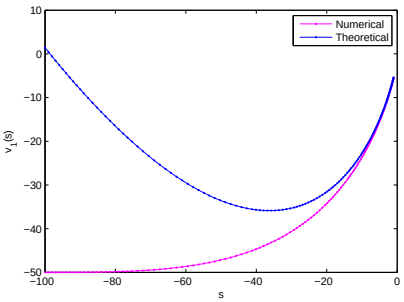

(d) $\gamma = 10$.

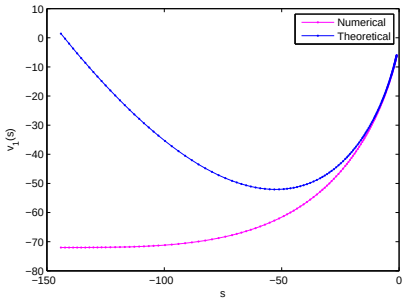

(e) $\gamma = 12$.

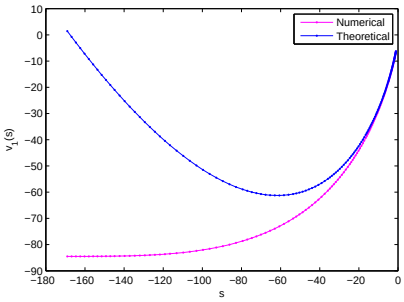

(f) $\gamma = 13$.

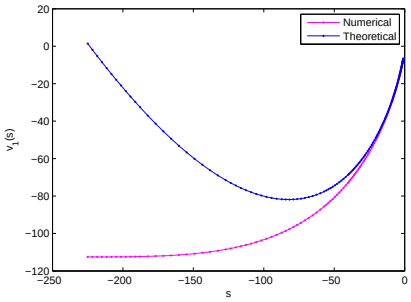

(g) $\gamma = 15$.

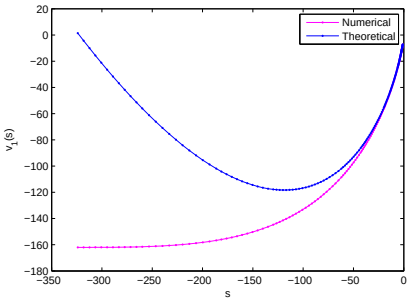

(h) $\gamma = 18$.

Figure 11: Analytical values and numerical approximation for v_1, order 8.

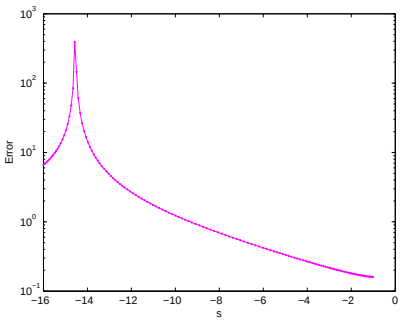

(a) $\gamma = 4$.

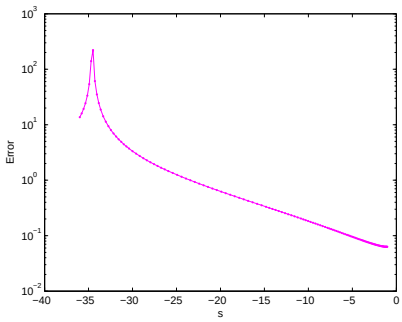

(b) $\gamma = 6$.

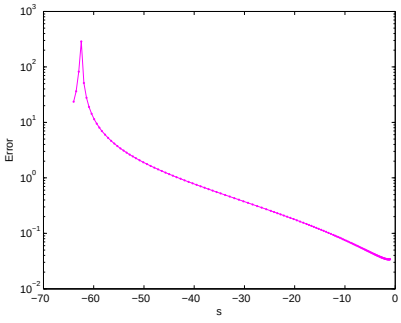

(c) $\gamma = 8$.

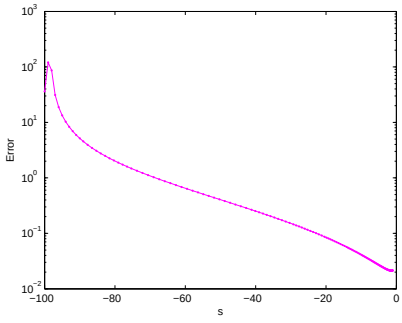

(d) $\gamma = 10$.

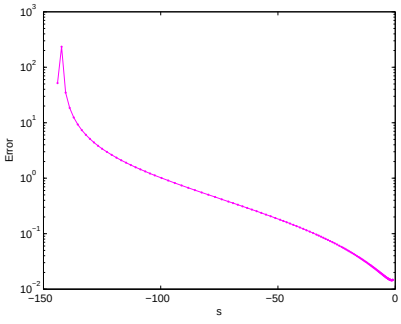

(e) $\gamma = 12$.

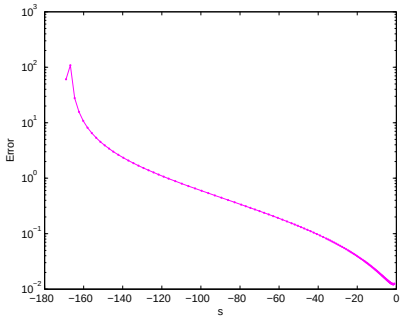

(f) $\gamma = 13$.

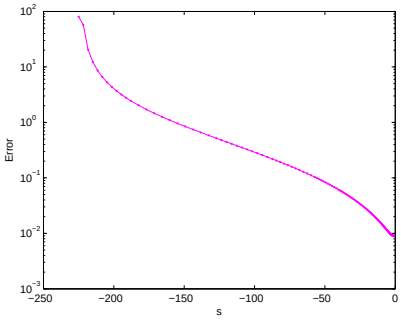

(g) $\gamma = 15$.

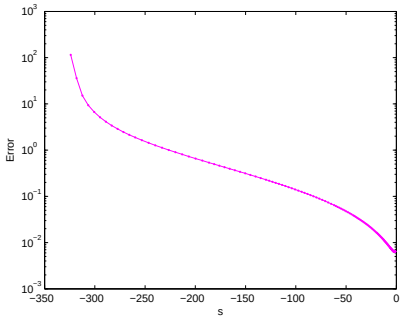

(h) $\gamma = 18$.

Figure 12: Relative error of v_1, order 8.

5 Asymptotical properties: Part 3 – Mid-range calculations, $s > 0$

To complete our discussion of the mid-range, we consider positive s.
Case 2: $1 \ll |s| \ll \gamma^2, \quad s > 0$

Let $1 \ll s \ll \gamma^2$. We recall that

$$y(s) = \frac{s}{\gamma^3} + \frac{1}{\gamma}, \quad s = \gamma^3 y - \gamma^2, \tag{18}$$

and

$$v_\infty = \gamma^4 \theta_\infty, \quad v(s) = \gamma^4 \theta(y). \tag{19}$$

For the numerical simulation, we again choose points y such that s is in the interval $[1, \gamma^2]$, i.e., $\frac{1}{\gamma} + \frac{1}{\gamma^3} \ll y \ll \frac{2}{\gamma}$ and calculate $\theta(y)$.

The asymptotic values of $v(s)$ are given in [7] as

$$v(s) = v_\infty \left(1 + e^{-\gamma_e} e^{-(s-s^*)/v_\infty}\right), \tag{20}$$

where $s^* = \frac{1}{2} + O(1/\gamma^2)$ and $\gamma_e = 0.577215665$ is Euler's constant. For large value of γ the value of v_∞ is very small, and therefore, $v(s)$ in (20) is nearly constant and coincides with v_∞.

Concerning the derivative $v_s(s)$ of $v(s)$, from (18) we obtain

$$y'(s) = \frac{1}{\gamma^3}, \tag{21}$$

and it follows from (19) that

$$v_s(s) = \gamma^4 \theta_y(y(s)) y'(s) = \frac{\gamma^4}{\gamma^3} \theta_y(y) = \gamma \theta_y(y). \tag{22}$$

Now, it is clear that for $s \in [1, \gamma^2]$, $y \in \left[\frac{1}{\gamma} + \frac{1}{\gamma^3}, \frac{2}{\gamma}\right]$, and using (18) we obtain the numerical approximation for the value of $v_s(s)$ from (22).

Finally,

$$v_s(s) = -e^{-\gamma_e} e^{-(s-s^*)/v_\infty} \tag{23}$$

holds [7], where $s^* = \gamma^3 y^* - \gamma^2$, and $\gamma_e = 0.577215665$.

In Figures 13 to 18, we give the graphs of $v(s)$ and the relative error (in logarithmic scale) obtained from (19) and (20).
Unfortunately, due to the very large values of v_∞, the numerical values of $e^{-(s-s^*)/v_\infty}$ are zero and consequently, the values of $v_s(s)$ obtained from (23)

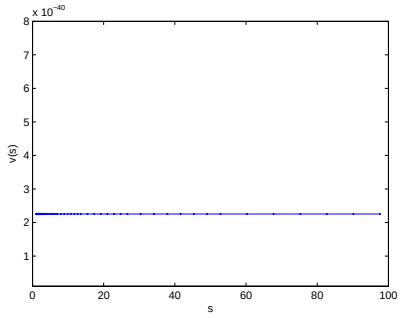

(a) $v(s)$, $v_\infty = 2.254440321030589e-040$.

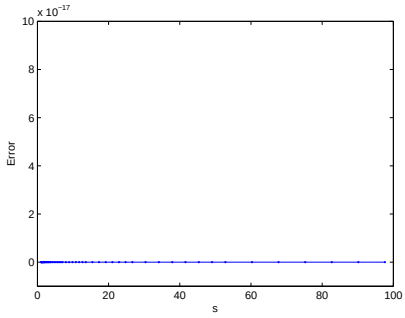

(b) Relative error of $v(s)$.

Figure 13: $\gamma = 10$, order 4.

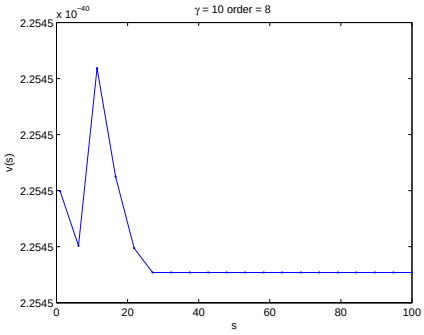

(a) $v(s)$, $v_\infty = 2.254439903035485e-040$.

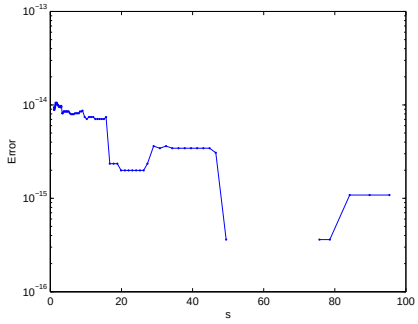

(b) Relative error of $v(s)$.

Figure 14: $\gamma = 10$, order 8.

are also zero.

In Figures 19 to 24, we give the graphs of $v(s)$ and $v_s(s)$ and also their absolute errors obtained from (19) and (20), and from (22) and (23), respectively.

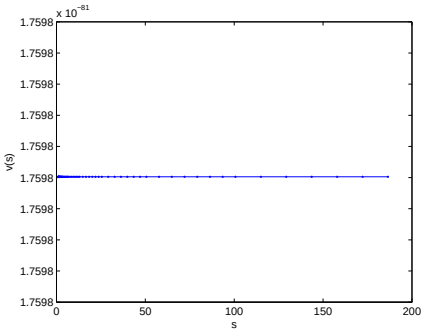

(a) $v(s)$, $v_\infty = 1.759790718101318e-081$.

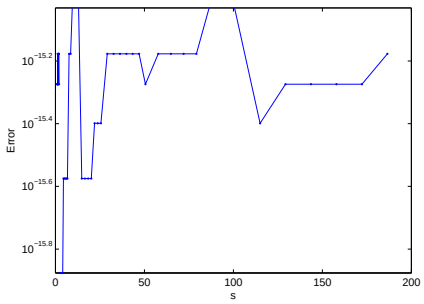

(b) Relative error of $v(s)$.

Figure 15: $\gamma = 14$, order 4.

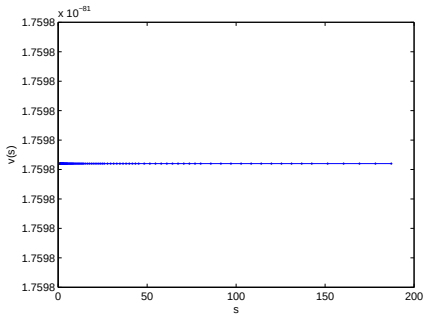

(a) $v(s)$, $v_\infty = 1.759789734510082e-081$.

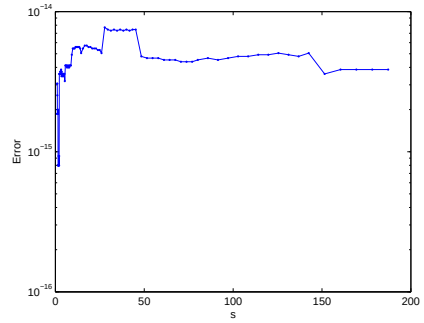

(b) Relative error of $v(s)$.

Figure 16: $\gamma = 14$, order 8.

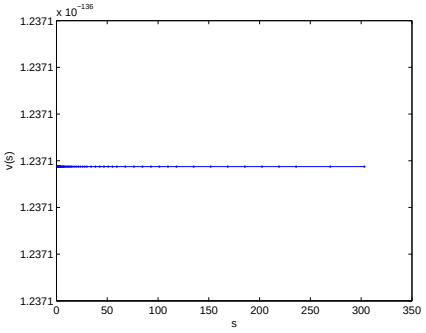

(a) $v(s)$, $v_\infty = 1.237140784693673e-136$.

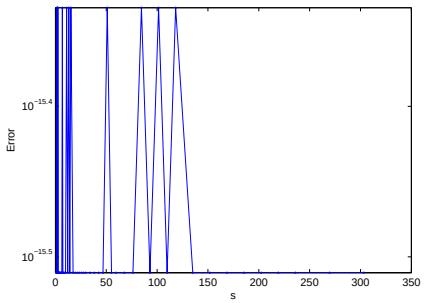

(b) Relative error of $v(s)$.

Figure 17: $\gamma = 18$, order 4.

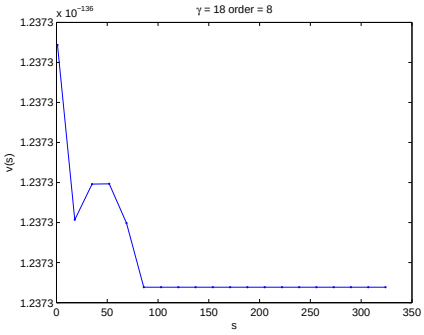

(a) $v(s)$, $v_\infty = 1.237139261913018e - 136$.

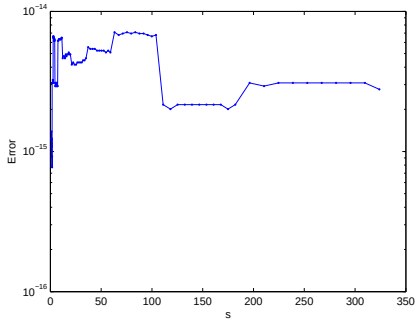

(b) Relative error of $v(s)$.

Figure 18: $\gamma = 18$, order 8.

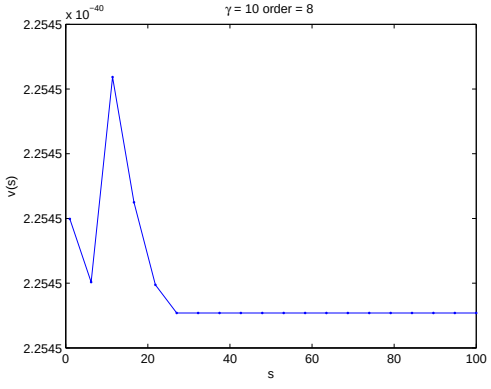

(a) $v(s)$, $\max_s |v(s)| = 2.254510924061732e - 040$

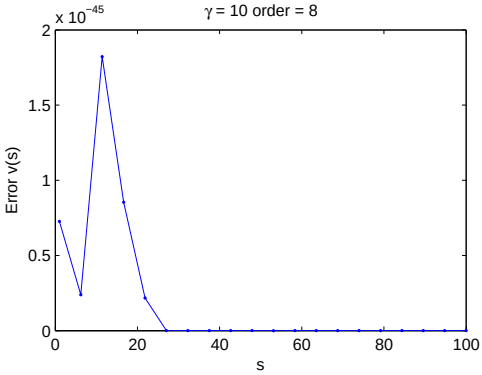

(b) Absolute error of $v(s)$

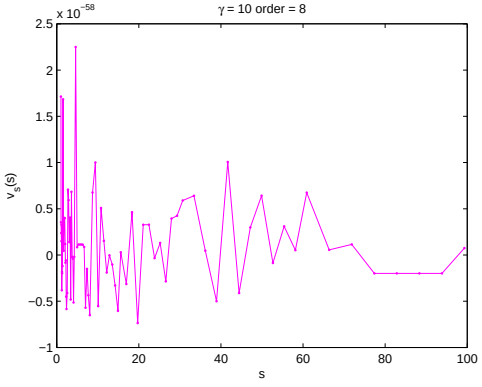

(c) $v_s(s)$, $\max_s |v_s(s)| = 2.249177359653094e - 058$

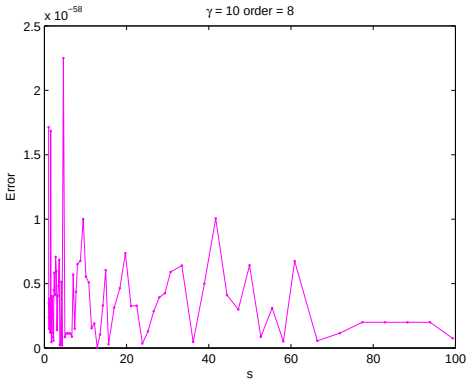

(d) Absolute error of $v_s(s)$

Figure 19: $\gamma = 10$, order 8

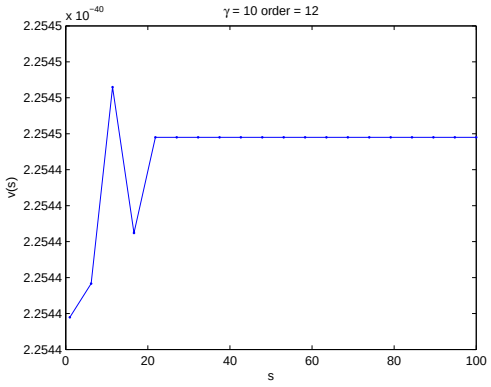

(a) $v(s)$, $\max_s |v(s)| = 2.254450648515892e-040$

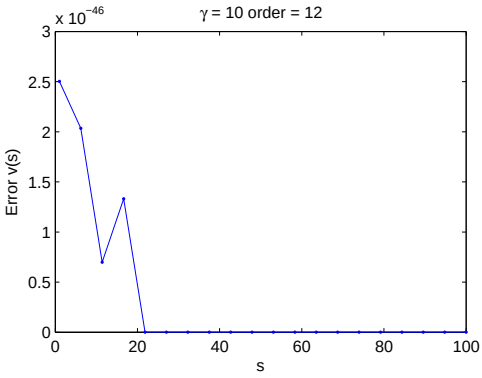

(b) Absolute error of $v(s)$

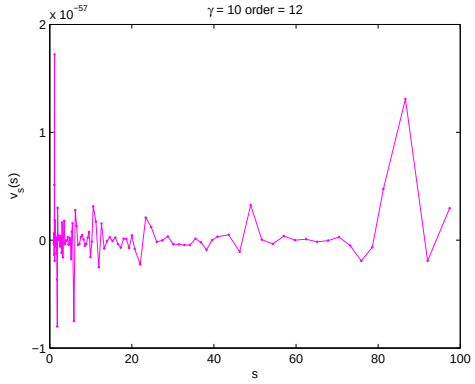

(c) $v_s(s)$, $\max_s |v_s(s)| = 1.722282721442703e-057$

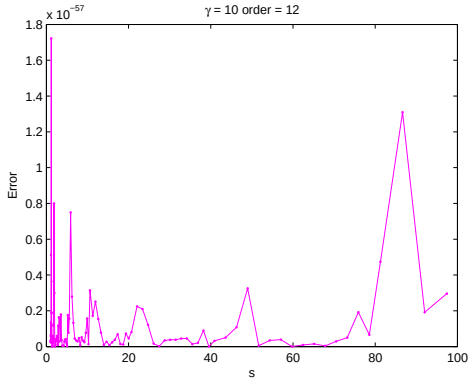

(d) Absolute error of $v_s(s)$

Figure 20: $\gamma = 10$, order 12

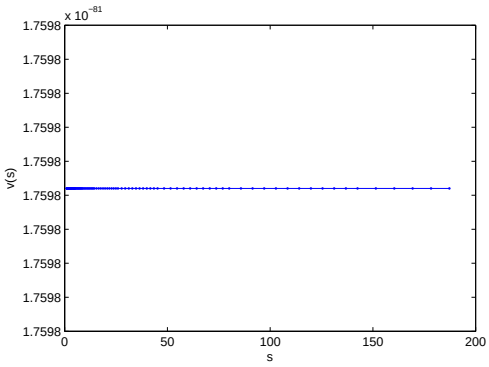

(a) $v(s)$, $\max_s |v(s)| = 1.759935454138890e-081$

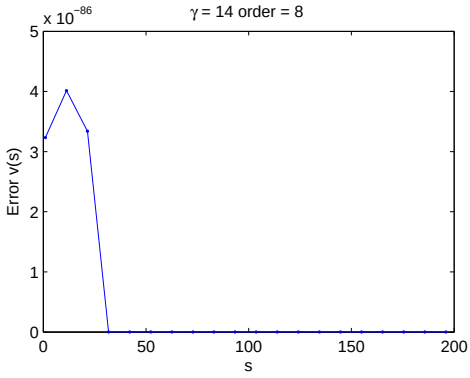

(b) Absolute error of $v(s)$

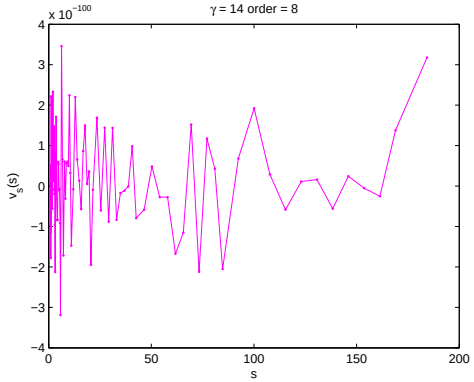

(c) $v_s(s)$, $\max_s |v_s(s)| = 3.458216725185613e-100$

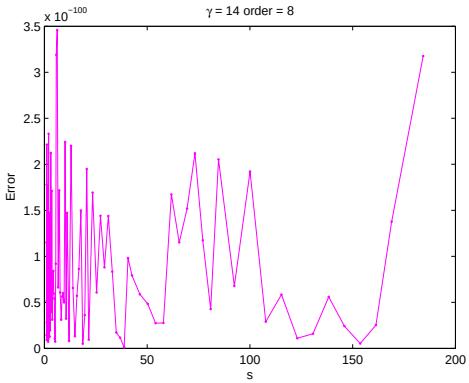

(d) Absolute error of $v_s(s)$

Figure 21: $\gamma = 14$, order 8

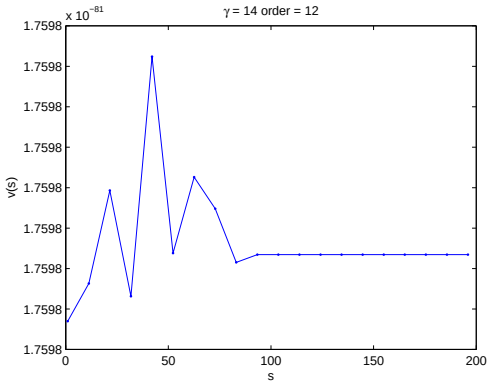

(a) $v(s)$, $\max_s |v(s)| = 1.759822479292100e-081$

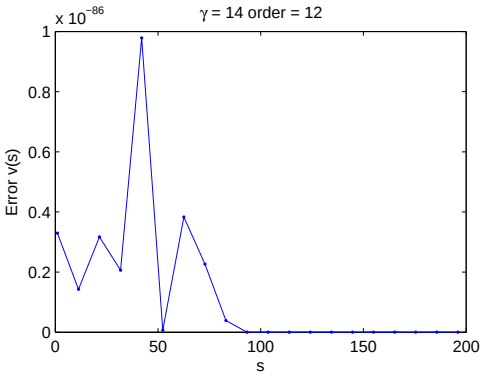

(b) Absolute error of $v(s)$

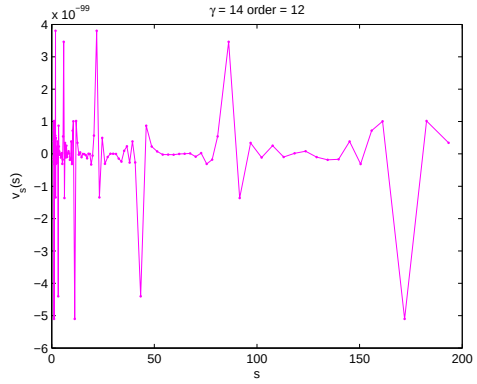

(c) $v_s(s)$, $\max_s |v_s(s)| = 5.098561192338281e-099$

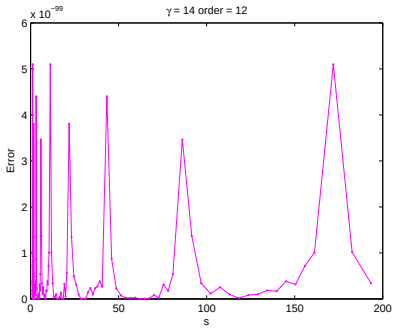

(d) Absolute error of $v_s(s)$

Figure 22: $\gamma = 14$, order 12

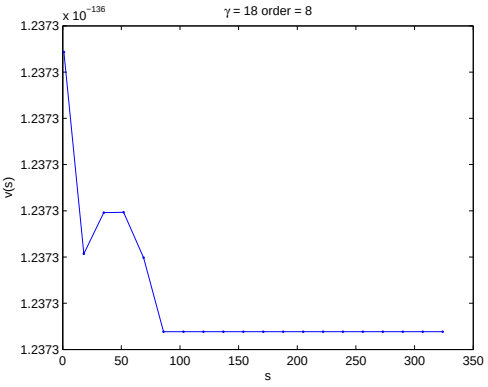

(a) $v(s)$, $\max_s |v(s)| = 1.237327181687361e-136$

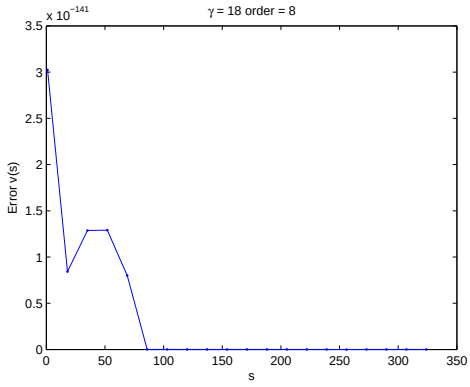

(b) Absolute error of $v(s)$

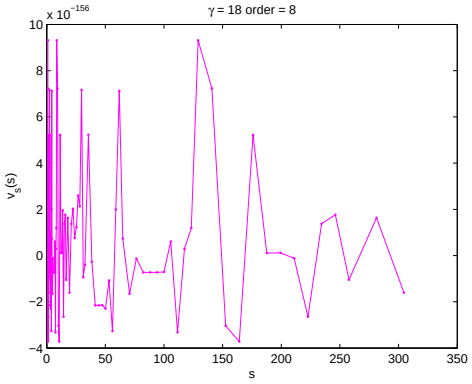

(c) $v_s(s)$, $\max_s |v_s(s)| = 9.313541238871319e-156$

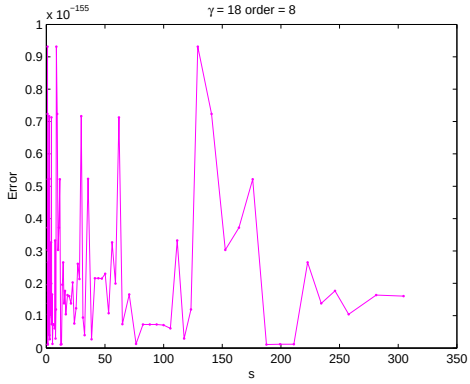

(d) Absolute error of $v_s(s)$

Figure 23: $\gamma = 18$, order 8

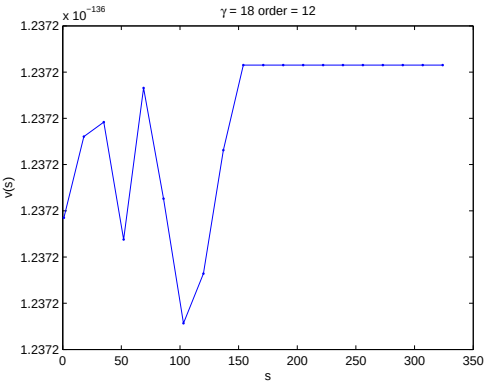

(a) $v(s)$, $\max_s |v(s)| = 1.237205762448720e - 136$

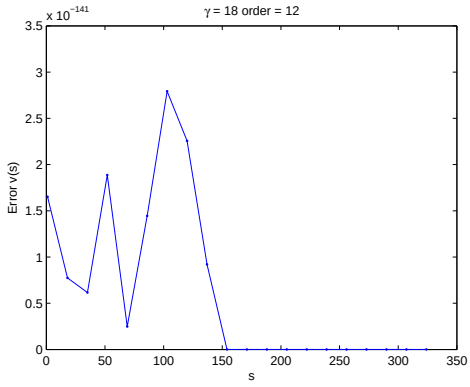

(b) Absolute error of $v(s)$

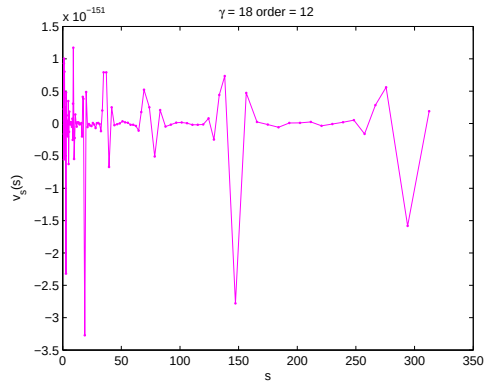

(c) $v_s(s)$, $\max_s |v_s(s)| = 3.271253987750634e - 154$

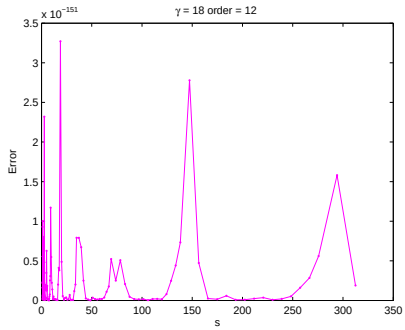

(d) Absolute error of $v_s(s)$

Figure 24: $\gamma = 18$, order 12

6 Numerical Method

In this section, we describe the finite difference method used in the computations. The numerical scheme is applied to second-order initial value problems in their original formulation. It is carried out on piecewise equidistant grids, where step size is changed after each subinterval, as proposed in the general block–BVM framework [5].
Let us consider a general second order initial value problem of the form

$$\begin{cases} f(y, \theta, \theta', \theta'') = 0, \\ \theta(y_0) = \theta_0, \quad \theta'(y_0) = \theta'_0. \end{cases} \tag{24}$$

Let h_0 be an initial step size and

$$Y = \{y_0 < y_1 < \ldots < y_n,\, y_i = y_0 + ih_0,\, i = 0, \ldots, n\}$$

an equidistant grid. The corresponding numerical approximation is denoted by

$$\Theta = [\theta_0,\ \theta_1,\ \ldots,\ \theta_n].$$

Following ideas from [2, 3, 4], we discretize the derivatives in (24) by means of suitably chosen high order finite differences

$$\theta^{(\nu)}(y_i) \simeq \theta_i^{(\nu)} = \frac{1}{h^\nu} \sum_{j=-s}^{r} \alpha_{s+j}^{(s,\nu)} \theta_{i+j} \tag{25}$$

where $\nu = 1, 2$ is the derivative index and $\alpha_{s+j}^{(s,\nu)}$ are the coefficients of the method which are specified in order to reach the possibly high order of accuracy. The integers s and r represent the number of left and right values required to approximate $\theta^{(\nu)}(y_i)$. They are strongly related to the convergence order and the stability properties of the formula. For the above problem we choose, $r = s$, whenever possible and obtain formulae called ECDF in [4] whose consistency order is $p = 2s$ for both, the first and the second derivative. For example, we have for

Order 4:

$$h^2\ \theta''(y_i) \approx -\tfrac{1}{12}\theta_{i-2} + \tfrac{4}{3}\theta_{i-1} - \tfrac{5}{2}\theta_i + \tfrac{4}{3}\theta_{i+1} - \tfrac{1}{12}\theta_{i+2},$$
$$h\ \theta'(y_i) \approx \tfrac{1}{12}\theta_{i-2} - \tfrac{2}{3}\theta_{i-1} + \tfrac{2}{3}\theta_{i+1} - \tfrac{1}{12}\theta_{i+2},$$

Order 6:

$$h^2\ \theta''(y_i) \approx \tfrac{1}{90}\theta_{i-3} - \tfrac{3}{20}\theta_{i-2} + \tfrac{3}{2}\theta_{i-1} - \tfrac{49}{18}\theta_i + \tfrac{3}{2}\theta_{i+1} - \tfrac{3}{20}\theta_{i+2} + \tfrac{1}{90}\theta_{i+3},$$
$$h\ \theta'(y_i) \approx -\tfrac{1}{60}\theta_{i-3} + \tfrac{3}{20}\theta_{i-2} - \tfrac{3}{4}\theta_{i-1} + \tfrac{3}{4}\theta_{i+1} - \tfrac{3}{20}\theta_{i+2} + \tfrac{1}{60}\theta_{i+3}.$$

We observe that the coefficients are symmetric and skew-symmetric for the second and first derivatives, respectively. In the computations, we have used these

schemes up to order $p = 10$.

The vector of unknowns Θ is computed by solving the nonlinear system of equations

$$f(y_i, \theta_i, \theta_i^{(1)}, \theta_i^{(2)}) = 0, \qquad i = 1, \ldots, n-1, \tag{26}$$

together with initial conditions. Since the above symmetric formulae of order $p > 2$ cannot be used to approximate $\theta^{(\nu)}(y_i)$, $i = 1, \ldots, p/2 - 1$ and $i = n - p/2 + 1, \ldots, n - 1$, schemes in (25) with different stencils (but the same consistency order) have to be provided at the beginning and the end of the grid. We call them initial and final formulae [5]. Examples of the initial schemes are

Order 4

$$\begin{aligned}
h^2\ \theta''(y_1) &\approx \frac{5}{6}\theta_0 - \frac{5}{4}\theta_1 - \frac{1}{3}\theta_2 + \frac{7}{6}\theta_3 - \frac{1}{2}\theta_4 + \frac{1}{12}\theta_5,\\
h\ \theta'(y_1) &\approx -\frac{1}{4}\theta_0 - \frac{5}{6}\theta_1 + \frac{3}{2}\theta_2 - \frac{1}{2}\theta_3 + \frac{1}{12}\theta_4.
\end{aligned}$$

Order 6

$$\begin{aligned}
h^2\ \theta''(y_1) &\approx \frac{7}{10}\theta_0 - \frac{7}{18}\theta_1 - \frac{27}{10}\theta_2 + \frac{19}{4}\theta_3 - \frac{67}{18}\theta_4 + \frac{9}{5}\theta_5 - \frac{1}{2}\theta_6 + \frac{11}{180}\theta_7,\\
h^2\ \theta''(y_2) &\approx -\frac{11}{180}\theta_0 + \frac{107}{90}\theta_1 - \frac{21}{10}\theta_2 + \frac{13}{18}\theta_3 + \frac{17}{36}\theta_4 - \frac{3}{10}\theta_5 + \frac{4}{45}\theta_6 - \frac{1}{90}\theta_7,\\
h\ \theta'(y_1) &\approx -\frac{1}{6}\theta_0 - \frac{77}{60}\theta_1 + \frac{5}{2}\theta_2 - \frac{5}{3}\theta_3 + \frac{5}{6}\theta_4 - \frac{1}{4}\theta_5 + \frac{1}{30}\theta_6,\\
h\ \theta'(y_2) &\approx \frac{1}{30}\theta_0 - \frac{2}{5}\theta_1 - \frac{7}{12}\theta_2 + \frac{4}{3}\theta_3 - \frac{1}{2}\theta_4 + \frac{2}{15}\theta_5 - \frac{1}{60}\theta_6.
\end{aligned}$$

The final schemes used to approximate $\theta^{(\nu)}(y_n)$ and, for order 6, $\theta^{(\nu)}(y_{n-1})$, have the same coefficients as the above initial ones, but in case of the first derivative, having reversed order and opposite signs. Note that for the second derivative, the order of the initial methods is $p = r + s - 1$, and so we need to include an additional grid point to obtain the required order $p = r + s$.
The number of grid points $n \geq p$ used while solving (26) is linked to stability and computational cost. Larger n means better stability properties but higher computational cost [2, 5]. For problem (24) we have $n =: p + 4$. The structure of the coefficient matrix associated with the second derivative for $p = 10$ is depicted in Figure 25. In this case, we included four initial and four final formulae, and five regular symmetric schemes [5]. The size of the matrix is $(n-1)\times(n+1)$, with the first column is multiplied by the known value of θ_0.

If A and B are the matrices containing the coefficients for the second and the first derivative, respectively. Then the discrete problem has the form

$$f\left(Y, \Theta, \frac{1}{h}B\Theta, \frac{1}{h^2}A\Theta\right) = 0, \tag{27}$$

where the first element of the vector Θ is known. System (27) combined with a formula approximating the first derivative $\theta'(y_0)$, obtained by (25) with $i = s = 0$, uniquely specifies the solution vector Θ. Examples of these last formulae are:

Order 4:

$$h\theta'(y_0) \approx -\tfrac{25}{12}\theta_0 + 4\theta_1 - 3\theta_2 + \tfrac{4}{3}\theta_3 - \tfrac{1}{4}\theta_4 = h\theta'_0,$$

Order 6:

$$h\theta'(y_0) \approx -\tfrac{49}{20}\theta_0 + 6\theta_1 - \tfrac{15}{2}\theta_2 + \tfrac{20}{3}\theta_3 - \tfrac{15}{4}\theta_4 + \tfrac{6}{5}\theta_5 - \tfrac{1}{6}\theta_6 = h\theta'_0.$$

Once the solution in the grid point y_i has been approximated, but its accu-

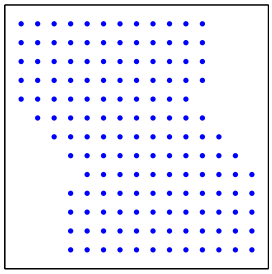

Figure 25: Structure of the coefficient matrix approximating the second derivative for $p = 10$ and $n = p + 4 = 14$.

racy is not sufficient to satisfy the tolerance requirements, the step size can be adapted on the basis of local error estimate obtained from the mesh halving strategy. Then the algorithm is continued on a subsequent subinterval. The code solving the *flow in concrete* problem uses a classical time stepping strategy [11] explained below.

If (Newton does not converge within $N_{\max}$ iterates)
$h = 0.8\,h$
elseif (error $> tol$)
$$h = \left(\frac{0.5\,tol}{\text{error}}\right)^{\frac{1}{(p+1)}} h$$
else
$$h_{\text{new}} = \left(\frac{0.7\,tol}{\text{error}}\right)^{\frac{1}{(p+1)}} h$$
end

In the first two cases the solution is not accepted and the algorithm restarts from the same point y_i. In the third case the solution is accepted and the new

step size h_{new} is predicted to handle the successive subinterval. The following table shows the number of Newton calls in which no converge has been observed within $N_{\max} = 10$ iterations. It also shows how often the tolerance has and has not been satisfied.

Statistics for order 8

	$\gamma = 4$	$\gamma = 10$	$\gamma = 18$
No convergence	0	0	1
error $>$ *tol*	57	336	1043
error $<$ *tol*	110	519	1554

The numerical results has been obtained with the following settings: Convergence orders $p = 2s$, $s = 2, 3, 4, 5$ initial step size $h_0 = 1e - 3$, error tolerance $tol = 1e - 12$ for both, the solution and the Newton residual.

References

[1] P. Amodio and G. Settanni. Variable step/order generalized upwind methods for the numerical solution of second order singular perturbation problems. *JNAIAM J. Numer. Anal. Indust. Appl. Math.*, 4:65–76, 2009.

[2] P. Amodio and G. Settanni. High order finite difference schemes for the solution of second order initial value problems. *JNAIAM J. Numer. Anal. Indust. Appl. Math.*, 5:3–16, 2010.

[3] P. Amodio and I. Sgura. High-order finite difference schemes for the solution of second-order BVPs. *J. Comput. Appl. Math.*, 176:59–76, 2005.

[4] P. Amodio and I. Sgura. High order generalized upwind schemes and numerical solution of singular perturbation problems. *BIT*, 47:241–257, 2007.

[5] L. Brugnano and D. Trigiante. *Solving Differential Problems by Multistep Initial and Boundary Value Methods*. Gordon and Breach Science Publishers, Amsterdam, 1998.

[6] W. Brutsaert. Universal constants for scaling the exponential soil water diffusivity. *Water Resour. Res.*, 15(2):481–483, 1979.

[7] C.J. Budd and J. Stockie. Asymptotic behaviour of wetting fronts in porous media with exponential moisture diffusivity. University of Bath report, University of Bath, 2012.

[8] Z. Chen, G. Huan, and Y. Ma. *Computational Methods for Multiphase Flows in Porous Media*. SIAM, Philadelphia, PA, 2006.

[9] B. E. Clothier and I. White. Measurement of sorptivity and soil water diffusivity in the field. *Soil Sci. Soc. Amer. J.*, 45:241–245, 1981.

[10] C. Leech, D. Lockington, and P. Dux. Unsaturated diffusivity functions for concrete derived from NMR images. *Mater. Constr.*, 34:413–418, 2003.

[11] W.H. Press, B.P. Flannery, S.A. Teukolsky, and W.T. Vetterling. *Numerical Recipes in C — The Art of Scientific Computing.* Cambridge University Press, Cambridge, U.K., 1988.

[12] M. Rose. Numerical methods for flows through porous media I. *Math. Comp.*, 40(162):435–467, 1983.